TWIST MODEL DEVELOPMENT AND RESULTS FROM THE ACTIVE AEROELASTIC WING F/A-18 AIRCRAFT

Andrew M. Lizotte and Michael J. Allen

NASA Dryden Flight Research Center
Bldg. 4876 Warehouse #6, Lilly Drive
Edwards, California 93523
e-mail: andrew.lizotte@mail.dfrc.nasa.gov and michael.allen@mail.dfrc.nasa.gov

Abstract. Understanding the wing twist of the active aeroelastic wing (AAW) F/A-18 aircraft is a fundamental research objective for the program and offers numerous benefits. In order to clearly understand the wing flexibility characteristics, a model was created to predict real-time wing twist. A reliable twist model allows the prediction of twist for flight simulation, provides insight into aircraft performance uncertainties, and assists with computational fluid dynamic and aeroelastic issues.

The left wing of the aircraft was heavily instrumented during the first phase of the active aeroelastic wing program allowing deflection data collection. Traditional data processing steps were taken to reduce flight data, and twist predictions were made using linear regression techniques. The model predictions determined a consistent linear relationship between the measured twist and aircraft parameters, such as surface positions and aircraft state variables. Error in the original model was reduced in some cases by using a dynamic pressure-based assumption. This technique produced excellent predictions for flight between the standard test points and accounted for nonlinearities in the data. This report discusses data processing techniques and twist prediction validation, and provides illustrative and quantitative results.

1 INTRODUCTION

This study investigates the process to determine and evaluate elastic streamwise twist predictions on the left wing of the active aeroelastic wing (AAW) aircraft. Understanding the wing twist onboard the AAW is a fundamental research objective for the program and offers numerous benefits. A reliable model allows the ability to predict twist in flight simulation, provides knowledge into aircraft performance uncertainties, and assists with computational fluid dynamic and aeroelastic issues.

The electro-optical flight deflection measurement system (FDMS) [1] was used to record absolute displacement at 16 different locations on the AAW left wing during phase-1 of the flight program. Resultant wing-twist time histories were calculated at four of the six available stations across the wingspan using the collected deflection data. The model objective was to predict measured twist using a multiple linear regression technique based on aircraft state variable and surface position characteristics. The following sections detail the process of creating a model to predict twist and determine technique reliability in twist predictions. Documentation includes the instrumentation setup, data acquisition and processing, and linear regression method used to develop the twist model. Other methods, such as a dynamic pressure-based assumption, were also used to further reduce error in original model twist predictions. Illustrative and quantitative results are presented for the model as well as analysis of anomalies and nonintuitive results.

2 BACKGROUND AND DATA PROCESSING

Analysis referred to in this report was performed with twist data measured on the AAW aircraft, a modified F/A-18 fighter as figure 1 shows. Changes on the aircraft to incorporate AAW technology include two major modifications [2]. Thinner panels replaced most top and bottom aft wing box panels, thereby increasing wing flexibility. This structural change made the AAW wing flexibility similar to that of original preproduction wings. Secondly, the inboard leading-edge flap (ILEF) and outboard leading-edge flap (OLEF) were decoupled to allow independent control of each surface. Typically, ILEFs and OLEFs are physically connected and must be controlled together. Separate controls and drives were implemented to control each leading-edge surface and allowed increased surface travel. These changes were the first stage in an effort to achieve the AAW program main objective to demonstrate roll control using wing twist. By integrating aerodynamics, flight controls, and structures, aeroelastic deformation of the wing may be used for a net benefit in roll control. Future aircraft designs using AAW research could enable higher aspect ratio and thinner and more flexible wings, which provide improved fuel efficiency from reduced aircraft weight and decreased aerodynamic drag. The AAW program is a joint effort between the Air Force Research Laboratory (AFRL, Edwards, California), Boeing's Phantom Works (St. Louis, Missouri), and NASA Dryden Flight Research Center (DFRC, Edwards, California).

Figure 1: AAW aircraft, modified F/A-18 fighter, 360-deg roll.

2.1 Instrumentation description

Vertical structural deflections of the AAW left wing were measured in flight using the FDMS. Figure 2(a) shows the 16 infrared light emitting diodes (LEDs) that were installed on the upper surface of the wing where the aeroelastically deformed surface could be measured. The targets were scanned sequentially beginning with target 0 and ending with target 15. Sequencing through the 16 LED targets took 80 ms, at which time the sequence began again with target 0, thus producing a sampling rate of 12.5 samples/s for each target. This sampling rate was adequate for quasi-static structural measurements, even for high-rate maneuvers such as abrupt step commands to the control surfaces [3].

Light from the target LED was focused as a line on a light-sensitive diode array mounted at the lens focal point. The receiver relayed to the control unit an electrical signal proportional to the point at which the target light encounters the diode array. Figure 2(b) shows an outboard view of the two optical receivers, which were mounted in the pod just aft of the cockpit to receive target data. A 10-cm focal length receiver was used to view inboard targets 0 through 9, while a 20-cm focal length receiver viewed outboard targets 10 through 15. Combining two receivers allowed complete field-of-view coverage and optimized resolution. The control unit, which contains logic necessary to operate the FDMS, also served to interface the FDMS with the pulse code

modulation (PCM) data-recording system. The deflection data were recorded as two 10-bit digital words. One word contained position data and the other word contained target identification and error messages. After acquired by the PCM system, data were transmitted to a ground station for recording. Previous applications of the FDMS technology include highly maneuverable aircraft technology (HiMAT) [4], X-29 forward-swept wing aircraft [3], advanced fighter technology integration (AFTI) F-111 mission adaptive wing research aircraft [5, 6], and F-16C Block 40 aircraft [7].
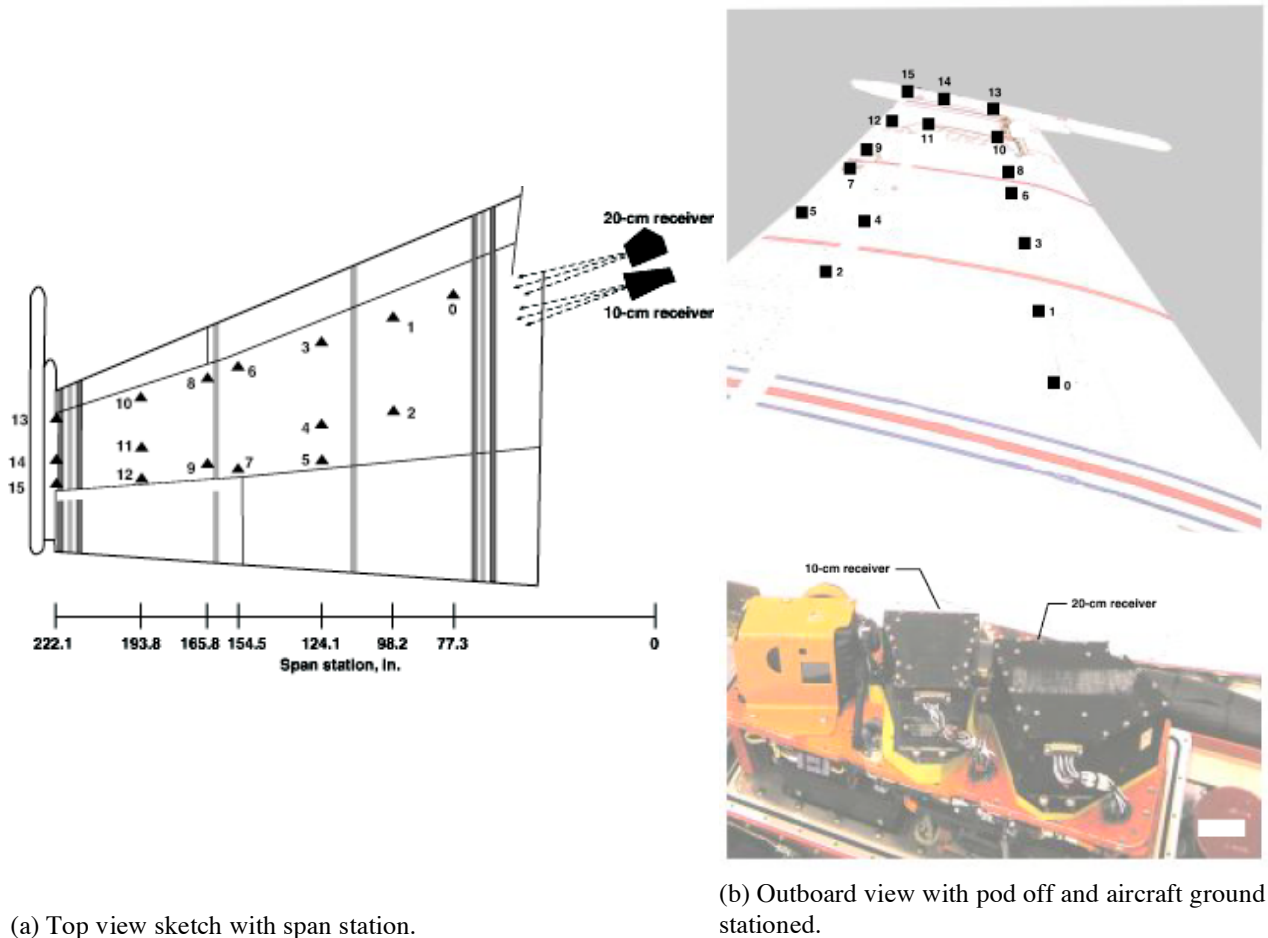

(a) Top view sketch with span station.

(b) Outboard view with pod off and aircraft ground stationed.

Figure 2: FDMS setup.

2.2 Instrumentation accuracy

With any measurement device, measurement precision is an important consideration. Figure 3 shows worst-case single scan deflection and twist resolution magnitudes for each twist station. These plots are derived from target-to-receiver distance, target-to-target chord length, and receiver focal length. Similar to the X-29 FDMS setup, the vertical field of view for each target was resolved into 1024 data counts. The broadest possible error band of a single measurement is ±2 counts. Calibration error may be reduced to approximately ±0.25 counts over the calibration range, making this error negligible on total measurement system accuracy. Trending the deflection or twist data throughout an interval of time allows the effective measurement error to approach zero. This minimally effective measurement error is caused by the calibration error yielding results much better than this worst-case plot.

As a result of using two receivers with different focal lengths, the corresponding pairing of targets to the receivers made the deflection resolution at span station 193.8 (fig. 2(a)) better than any other span. Figure 3 shows the twist resolution is also much better at span station 193.8,

whereas twist and deflection resolutions at span 165.8 are the worst. It is also important to mention that spans 154.5 and 222.1 possess nearly the same twist resolution.
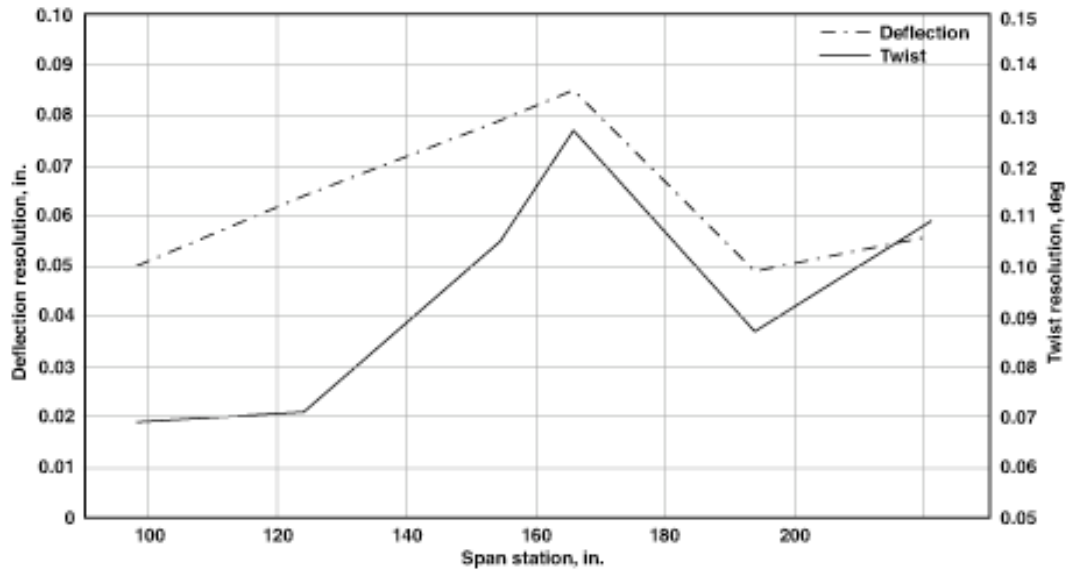
Figure 3: AAW FDMS deflection and twist resolution.

2.3 Project phase-1 objectives

From November 2002 through June 2003, the AAW program flew 51 phase-1 flights to accomplish the following objectives:

- Verify the ability of the baseline control law to fly the aircraft.
- Ensure all aircraft systems and instrumentation systems are functioning correctly.
- Characterize the F/A-18 aircraft test bed, its wings, and its control surfaces to quantify the effects of the wing system flexibility as a function of Mach and dynamic pressure.
- Understand the individual effectiveness of the control surfaces.
- Understand the wing box aeroelasticity as a control power-producing device across the flight test envelope.
- Understand how and where control reversal occurs for the AAW F/A-18 aircraft.

Table 1 shows the flight envelope to reach these objectives, which consisted of 18 primary flight conditions. Approximately 430 maneuvers were flown from the primary flight conditions and approximately 70 maneuvers were flown at intermediate conditions, for example Mach 0.93 at an altitude of 10,000 ft.

Altitude, ft	Mach					
	0.85	0.90	0.95	1.10	1.20	1.30
25,000				X	X	X
20,000				X	X	X
15,000	X	X	X	X	X	
10,000	X	X	X	X		
5,000	X	X	X			

Table 1: AAW phase-1 flight envelope.

Determination of control-surface effectiveness using parameter identification techniques [8] was performed with the use of the onboard excitation system (OBES) [9] to produce doublet maneuvers. Independent of the pilot, a predetermined schedule allowed the OBES to vary each control-surface position. Collective (symmetric control-surface excitation) and differential (asymmetric control-surface excitation) doublet maneuvers were performed for each control surface in a buildup approach from low-to high-magnitude deflections. Figure 4 illustrates a

small differential doublet control-surface deflection time history. Table 2 shows deflections for small, medium, and large collective OBES maneuvers and table 3 shows similar data for differential OBES maneuvers.
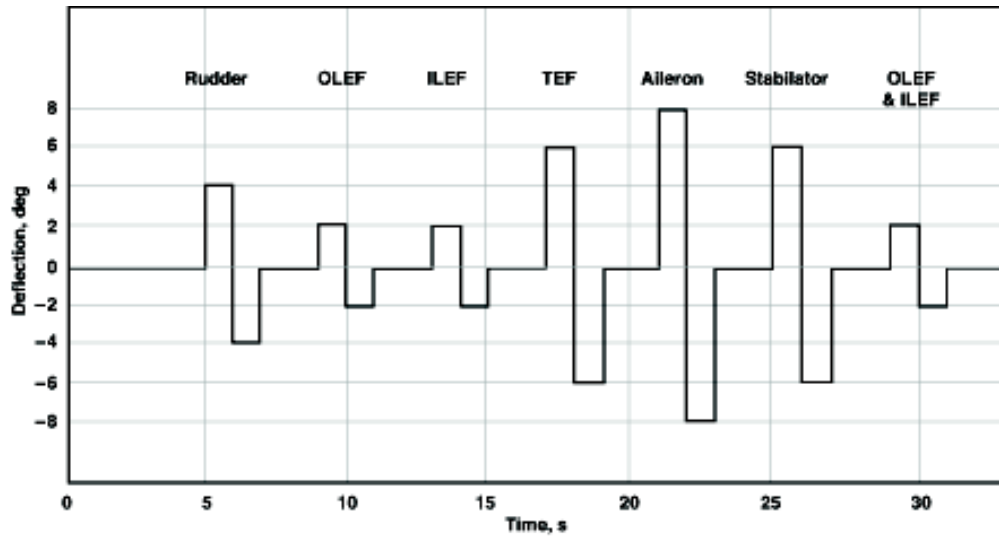

Figure 4: Small differential doublet control-surface deflection time history.

OBES Reference	OLEF	ILEF	TEF	OLEF and ILEF	Aileron	Stabilator
Large	3	3	5	3	6	0.8
Medium	2	2	4	2	5	0.8
Small	1	1	3	1	4	0.8

* Numerical values are represented in degrees.

Table 2: Collective OBES doublet maneuvers for parameter identification.*

OBES Reference	Rudder	OLEF	ILEF	TEF	Aileron	Stabilator	OLEF and ILEF
Large	4	6	6	10	12	6	6
Medium	4	4	4	8	10	6	4
Small	4	2	2	6	8	6	2

* Numerical values are represented in degrees.

Table 3: Differential OBES doublet maneuvers for parameter identification.*

To evaluate the linearity assumed in the twist model derived from standard OBES maneuvers, which produce low-twist levels only, additional maneuvers were required. Full stick rolls, windup turns, rolling pull-outs, bank-to-bank rolls, and push-over pull-ups were also flown at each flight condition to improve twist model accuracy at high-twist levels. Approximately 370 maneuvers were used in the construction of the twist model.

2.4 Data processing

AAW phase-1 flight data underwent many data processing steps before the data could be used to create the twist model. The following technique was initially used to develop a loads model for the AAW phase-2 control laws (CLAWS) and was applicable to twist model development.
1. Find dropouts.
2. Time synchronize data.
3. Remove data spikes.
4. Filter noise.
5. Remove stale data.
6. Calculate new parameters.

In order to find dropouts, each time signal was checked for missing time points. If missing points were found, they were filled with interpolated points and all signals at that sample rate were filled with interpolation as well. This step was used to remove data dropout problems from further data conditioning steps, such as spike removal and filtering. All filled points were

5

marked and removed after filtering. The AAW aircraft data stream was provided with time tag parameters to help correlate measured signals in time. These time tags were used to correct flight data before use in twist model development. Signals that were sampled at 25 Hz (aircraft surfaces) used a time tag associated with those measurements on the 1553 bus. All other parameters were corrected with an embedded time signal. Since the 25-Hz data were reported at 20 Hz using a buffer, the time delay for these signals ranged greatly. Variation in time synchronization usually ranged from 30 through 70 ms. Data spikes were identified with a derivative method and manually removed with visual inspection. The technique allowed the user to identify spikes and replace them with linear interpolation. Filtering was accomplished using forward and backward low-pass Butterworth filters. Filter bandwidths were chosen to remove noise from the signal without distorting the signal. Surface positions were not filtered because these signals have low noise and because the filter sometimes added dynamics to the signal when attempting to filter a sharp OBES doublet. Additional time points from any oversampled time signal were tagged as invalid. These tagged points, plus dropouts found in step 1 and spikes found in step 3, were removed from the data set in step 5. This removal was possible because the twist model is time invariant. Synthesized parameters were calculated from flight measurements to improve model accuracy. These parameters usually included the product of two parameters. Although 70 of these new parameters were created, the final twist model only uses a select few.

2.5 Twist calculation

Figure 5 illustrates angle of twist, θ, at the wingtip from vertical displacement difference, Δ, of TGT13 (target 13) and TGT15 (target 15). Fixed distance (chordwise spacing) between the two target locations is represented by δ. Actual twist may be calculated as $\theta = \sin^{-1}(\Delta / \delta)$. Though the FDMS arrangement allowed for twist calculation at six stations along the left wingspan, the outermost four stations were chosen for model development because of their high-twist output. Figure 6 shows these stations, referred to as FTWIST3 through FTWIST6.
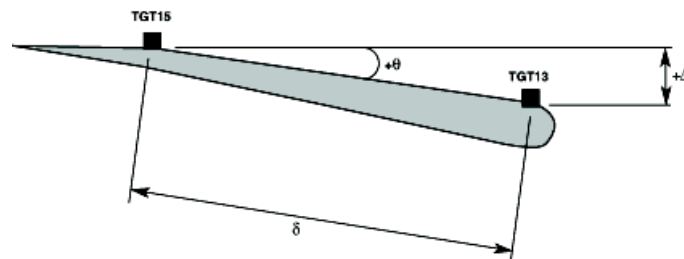

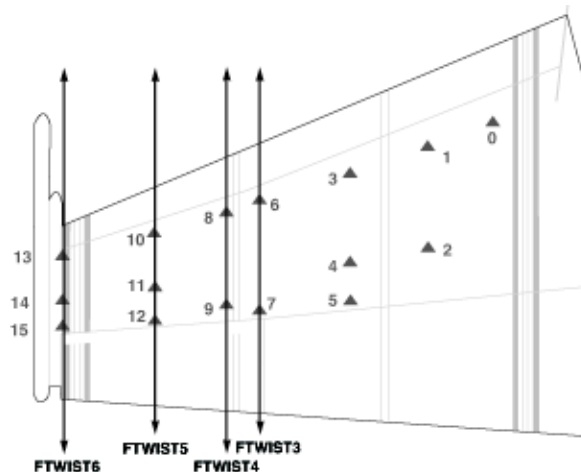Figure 5: Wingtip twist variables.

Figure 6: Modeled twist stations.

3 MODEL DEVELOPMENT

Model creation began by using an inhouse linear regression tool called EQuation DErivation (EQDE) [10]. Predictions were developed at each of the 4 twist stations at all 18 primary flight conditions using the majority of maneuvers. A specified number of maneuvers at each flight condition were not used in model formation, but as an independent check of the model performance. After model completion, a database was created to document the twist equations and aid implementation into the AAW simulator. Figure 7 shows the original model flowchart for one twist station at one flight condition.
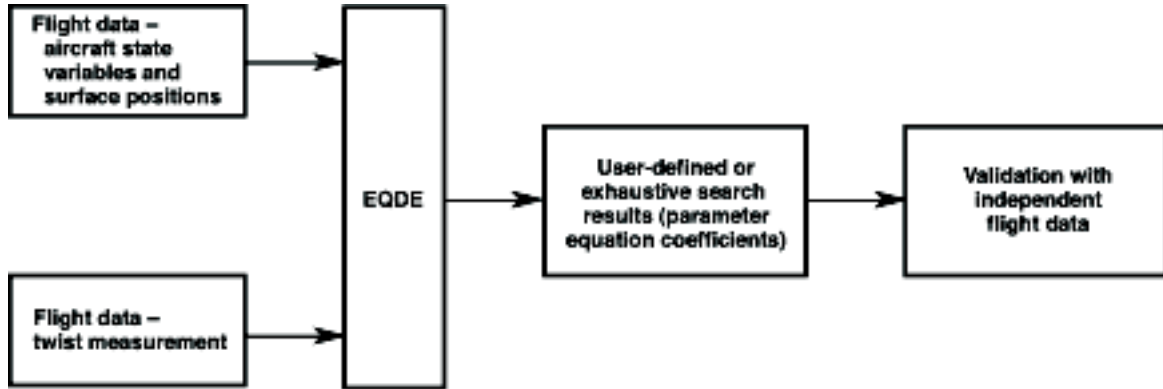

Figure 7: Original model flowchart.

Traditionally, EQDE has been used to facilitate the process of deriving loads equations from large quantities of strain gage data collected from loads calibration tests. In this case, EQDE was used to assist in the development of twist equations using large quantities of flight data from AAW phase-1 flights. The first of two primary EQDE functions was the calculation of twist influence coefficients and other statistical information for each maneuver. The influence coefficient was a measure of the correlation between parameter signal and twist undergone by the structure. Generally, parameters having larger influence coefficients produced better results. Secondly, EQDE derived equation coefficients from a given set of independent variables (aircraft state variables and surface positions, hereinafter referred to as simply 'parameter inputs') and a dependent variable (twist). The equation coefficients were then used to calculate twist for the model,

$$\text{Twist} = I + \sum_{i=1}^{n} P_i C_i \qquad (1)$$

where n is the number of parameter inputs, C_i is the equation coefficient for the ith parameter input, I is the intercept, and P_i is the ith model parameter input. Equation (1) calculates a single twist at a single point in time, making the twist model time invariant.

Two approaches to run EQDE were used to attain the influence and equation coefficients. The user either explicitly specified which parameter inputs to use in the equation or the user allowed EQDE to perform an exhaustive search. The exhaustive search analyzed all possible parameter input combinations to yield an equation with a constant twist relationship relative to a specified set of parameter inputs. Both approaches were used in analysis to determine the lowest error and most reliable prediction.

The EQDE output evaluation consisted of error analysis of validation maneuvers and evaluation of measured-to-predicted time history plots. Approximately 15 percent of the maneuvers from

any given flight condition were not used to create the model, but were reserved for use as an impartial check. Often, a high-twist maneuver (roll at 100-percent lateral control stick input) was used to train the model and a lower twist maneuver (roll at 50-percent stick input) was used to validate.

After deriving equations for the four twist stations at each of the flight conditions, a database was created to document the model intercept and coefficient terms. Aside from an ordered documentation of the model results, the database was used for preflight twist analysis within the simulator. Each twist station was described by one line of the twist model database. The twist model database indicated each flight condition as well as parameter input names, intercept, and model coefficients for each twist station. Table 4 is a section of the twist model database. The database lines define twist models for twist stations 3 through 6 (FTWIST3 through FTWIST6) at the flight condition of Mach 0.85 at an altitude of 15,000 ft (abbreviated as 085m15k). The intercept for the twist station 3 twist equation is 42.84. The same row gives all other model coefficients for the twist station 3 equation. Parameter inputs not used in the final equation for twist station 3 (Mach and Altitude) are set to zero.

085m15k

	Intercept	Mach	Altitude	Velocity	LAilLVDT	Alpha	Beta
FTWIST3	4.2840E+001	0.0000E+000	0.0000E+000	0.0000E+000	0.0000E+000	8.9110E+001	0.0000E+000 ...
FTWIST4	−2.2301E+001	0.0000E+000	0.0000E+000	0.0000E+000	0.0000E+000	0.0000E+000	−4.9660E+000 ...
FTWIST5	−6.2801E+001	0.0000E+000	0.0000E+000	0.0000E+000	0.0000E+000	0.0000E+000	4.9660E+000...
FTWIST6	8.9110E+001	0.0000E+000	0.0000E+000	0.0000E+000	0.0000E+000	0.0000E+000	0.0000E+000...
.	.	.	.	.	.	.	.
.	.	.	.	.	.	.	.
.	.	.	.	.	.	.	.

Table 4: Sample of twist model database.

4 DYNAMIC PRESSURE ASSUMPTION

Independent of the original model described previously, this section describes an alternative technique for wing-twist prediction. The dynamic pressure assumption (DPA) method predicts twist based on the aircraft dynamic pressure state instead of specific flight condition used with the original model.

One of the drawbacks to the original model was reduced model accuracy when the flight condition was different than the design condition. In order for the model to predict (for example, Mach 1.22 at an altitude of 20,000 ft), either the bounds of models Mach 1.20 at an altitude of 20,000 ft and Mach 1.30 at an altitude of 20,000 ft must be opened or there would have to be interpolation between the two models. The former was the preferred technique and implemented within the manned flight simulator. Interpolation was not the preferred technique because of complexity and increased processing time.

Ability to monitor real-time twist, free of flight condition constraints, could be extremely beneficial. One all-encompassing equation based on measured aircraft dynamic pressure may achieve this monitoring ability. Besides ability to predict twist at any point, calculation using this single equation would decrease control room processing time by an order of magnitude. In order to determine this relationship, a limited DPA study was performed with supersonic data at six flight conditions with one twist station. Figure 8 shows a simple flowchart.
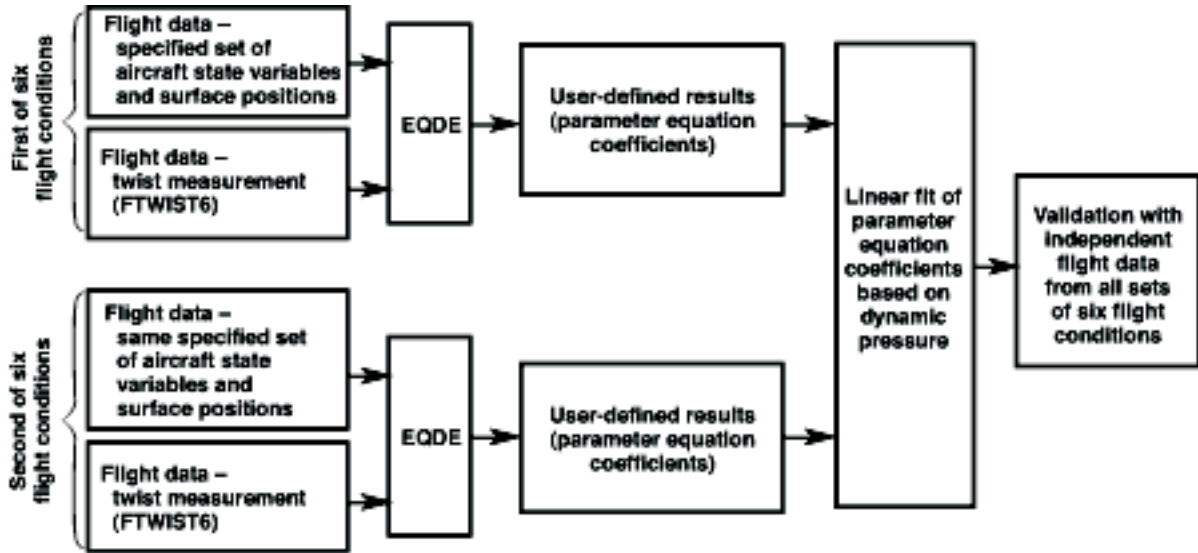
Figure 8: DPA flowchart.

Wingtip twist (FTWIST6) was modeled with EQDE at supersonic flight conditions in table 5 with constant parameter inputs. This supersonic, low dynamic pressure region was chosen because of the low error produced at the wingtip and the high quality of measured data. Parameter input equation coefficients were plotted compared with their corresponding dynamic pressure value to determine a linear relationship between the two. Figure 9 plots examples of a few parameter inputs compared with dynamic pressure. This plot shows a linear fit of the parameter inputs with dynamic pressure in grey and relative flight condition dynamic pressure on the x-axis.

Altitude, ft	Mach					
	0.85	0.90	0.95	1.10	1.20	1.30
25,000				X	X	X
20,000				X	X	X
15,000						
10,000						
5,000						

Table 5: DPA envelope.

Using this assumption, all of the maneuvers in the flight envelope (table 5) have an influence on the model, not just maneuvers from each flight condition as with the original model. The benefit is a data set from a broader pool of maneuvers, which may compensate for specific flight condition inadequacies. For example, all FDMS data from the 4-g rolling pull-out maneuvers at Mach 1.30 at an altitude of 25,000 ft were unusable because of poor flight data quality. This unsuitability appears to have little effect on the left outboard leading-edge flap rotary variable displacement transducer (LOLEFRVDT) position coefficient; however, the left aileron linear variable displacement transducer (LAilLVDT) position coefficient is far from the linear assumption. This method assumes, with ideal flight data at Mach 1.30 at an altitude of 25,000 ft, that the equation coefficient would be much closer to the linear fit. Equation (2) is used for this assumption.

$$\text{Twist}_{\text{DPA}} = C_t \bar{q} + I_t + \sum_{i=1}^{n} P_i (C_i \bar{q} + I_i) \qquad (2)$$

9

C_t is the equation intercept coefficient, I_t is the intercept coefficient, n is the number of parameter inputs, C_i and I_i are the equation coefficient and intercept for the ith parameter input, respectively, and P_i is the ith model parameter input. Equation (2) is similar to the original model equation; however, it is valid over the specified flight envelope as long as the dynamic pressure, $\bar{q}$, is known. The use of Cs and Is represent the slopes and intercepts of the linear fit of the parameter inputs plotted in figure 9.
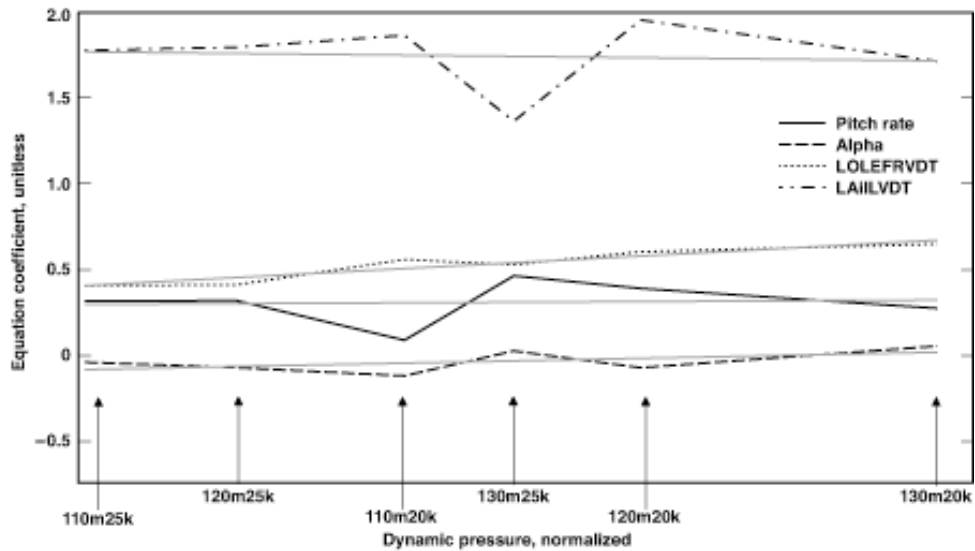

Figure 9: Equation coefficient compared with scaled dynamic pressure.

Using the previous example, a specific equation was determined at Mach 1.20 at an altitude of 20,000 ft, but valid from Mach 1.16 at an altitude of 20,000 ft through Mach 1.22 at an altitude of 20,000 ft. Although this technique allows twist prediction at virtually any Mach and altitude, flight at the boundary edge typically produced high error. Also, figure 10 shows that crossover from one boundary to the next creates a step in the data. The top plot displays a simulated slow acceleration followed by a brief deceleration with a Mach output range from 1.10 through 1.23 at an altitude of 20,000 ft. Original model boundaries as stated previously are indicated with a dash-dot line. As the Mach level passes these boundaries, the black trace on the bottom plot shows a step occurs with the original model. Independent of flight condition, the dashed trace shows DPA results indicate a smooth transition.
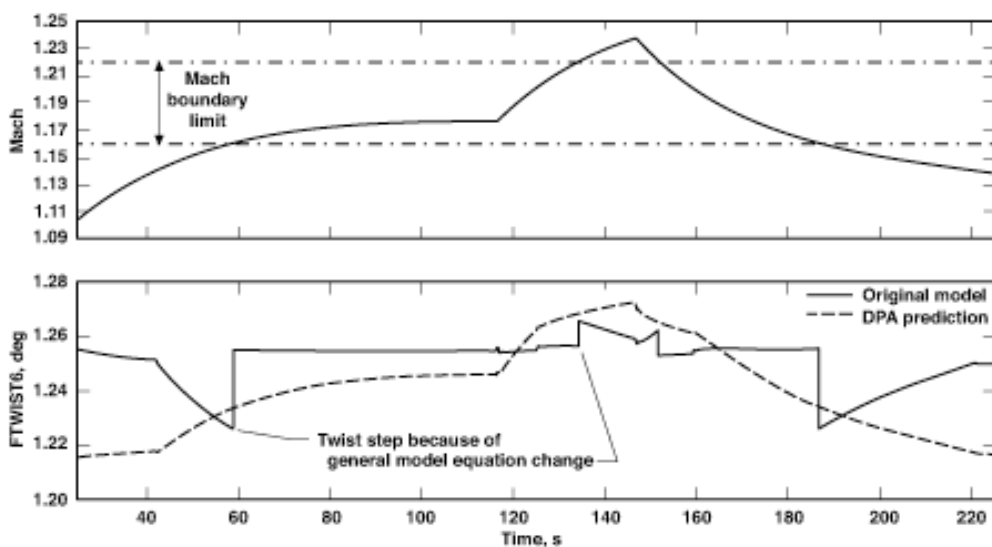

Figure 10: Original model wingtip twist step, 20,000 ft.

10

5 RESULTS

This section compares measured twists at the four stations with predicted twists from the original model and DPA. Although 18 primary flight conditions exist, results from specific maneuvers that represent a majority of twist behavior are presented.

As stated previously, individual control-surface effectiveness was determined with the use of doublet maneuvers at each flight condition. Figure 11 shows a typical small differential doublet maneuver and resultant measured wing twist at Mach 1.10 at an altitude of 20,000 ft. The top graph shows individual control-surface doublet deflection in degrees and the bottom graph illustrates absolute angle of twist in degrees of the wing at the four measured stations. Approximately 30 s of useful data from this maneuver is plotted. Twist measurement station values referenced to ground rest are shown as 0.4, 0.5, 0.8, and 1.1 for FTWIST3, FTWIST4, FTWIST5, and FTWIST6, respectively, at this flight condition. Twist magnitude increases spanwise from a maximum of about 0.9 at FTWIST3 through 1.9 at FTWIST6. From this maneuver, rudder doublet has virtually no direct linear relationship on wing twist, whereas combined inboard and outboard doublet has a significant effect on twist for minor control-surface deflection (2 deg). At each of the four twist stations, aileron doublet produced the highest overall twist and in general appears to have the most significant influence on twist.
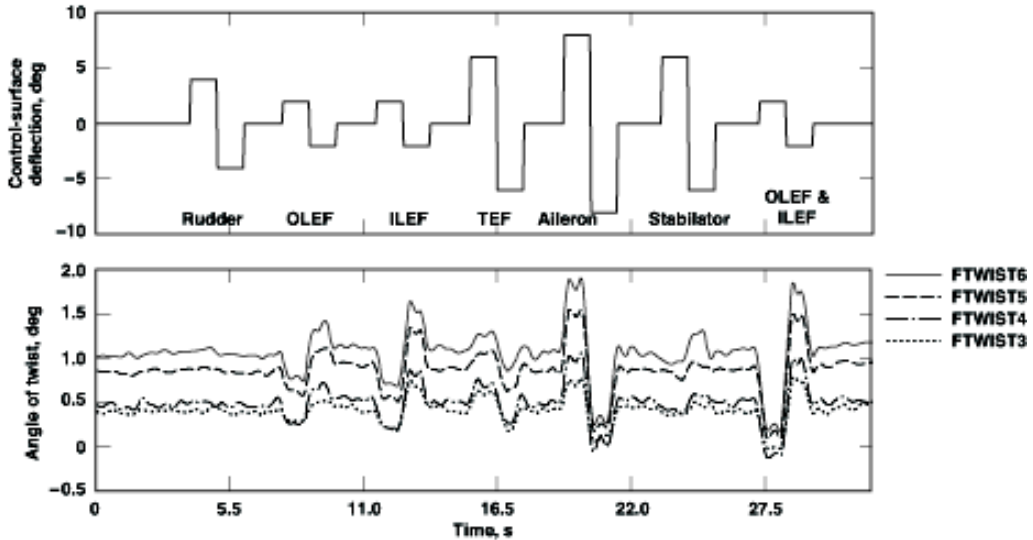

Figure 11: OBES doublet control-surface deflection and measured twist time history.

Establishment of signal to be modeled and influence of each control surface was not enough to produce reliable twist predictions. Intuition combined with EQDE exhaustive search capability allowed determination of the optimal set of control-surface positions and aircraft state variables. Typically, four main wing control surfaces (ILEF, OLEF, trailing-edge flap (TEF), and aileron) were used in concert with aircraft angle of attack, roll rate, and normal acceleration inputs to minimize error between original model predictions and measured twist.

Two metrics were used to quantify the original model results. The first metric was standard root mean square (RMS) error (eq. (3)),

$$\text{RMS} = \left[\frac{\sum\limits_{l=1}^{k} (M_l - R_l)^2}{k} \right]^{\frac{1}{2}} \qquad (3)$$

11

where k is the number of samples, M_l is the measured twist of sample number l, and R_l is the predicted twist of sample l. RMS error is one of the most commonly used statistical measures of success. The lower the RMS error, the more accurate the predicted trace follows that of the measured signal. The calculation allows each specific twist station to be individually compared throughout all flight conditions.
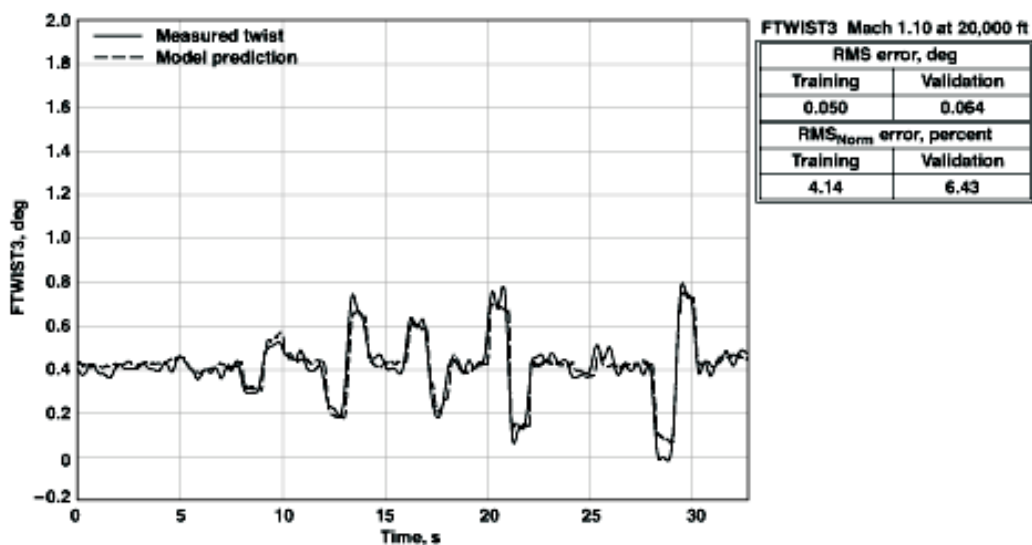
Another metric used to evaluate results is defined as the RMS error at a particular flight condition station divided by the twist angle range, T_{Range}, of the same station for that particular flight condition (eq. (4)).

$$\text{RMS}_\text{Norm} = \frac{\text{RMS}}{T_\text{Range}} \times 100 \tag{4}$$

This normalized percentage allows a direct comparison not only within flight conditions, but between twist stations as well. Once again, a lower RMS_Norm error indicates a strong correlation between measured and predicted signals.
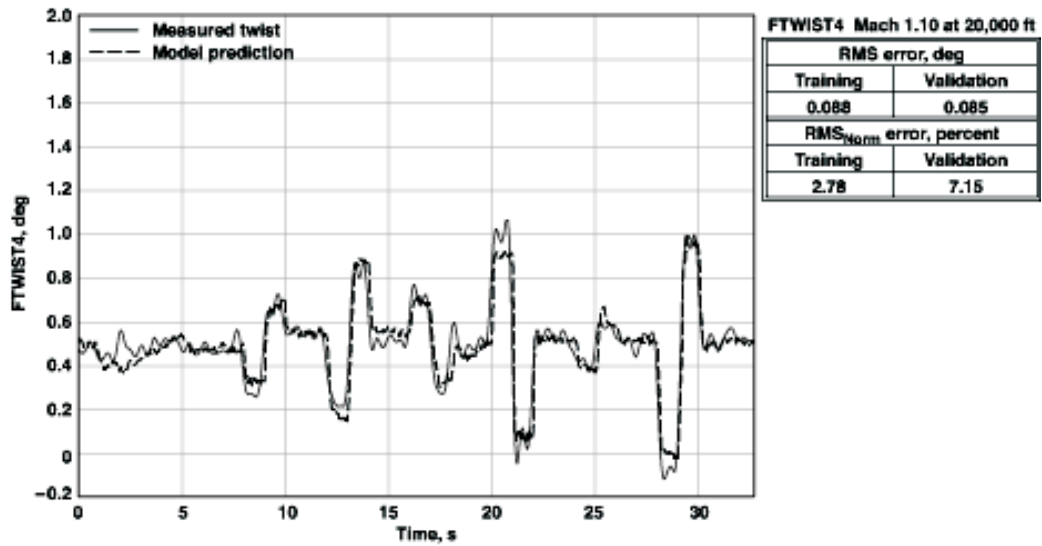
Figure 12 shows original model twist prediction results of the aforementioned small differential doublet. The figure illustrates measured absolute angle of twist and the corresponding twist prediction at the four twist stations. Model predictions in each plot were created from different optimal sets of parameter inputs based on EQDE results. Approximately 12 maneuvers at Mach 1.10 at an altitude of 20,000 ft were used to train the model and 3 maneuvers were used to validate the prediction.

Figure 12 also displays the two metrics discussed previously. The term *training* quoted in the marginal table of this figure refers to the metric calculated from the dozen maneuvers used to derive equation coefficients. This training error provides insight to the linearity of maneuvers used to create the model. The term *validation* quoted in the marginal table refers to the error calculated from the three maneuvers set aside as an independent check of the model. The validation error reflects how well the model predicts maneuvers from the same flight condition that were not used to create the model. Observation shows that the training error is greater than the validation error in some cases and is common because of the higher twist-producing maneuvers used for training.

FTWIST3 Mach 1.10 at 20,000 ft

RMS error, deg	
Training	Validation
0.050	0.064

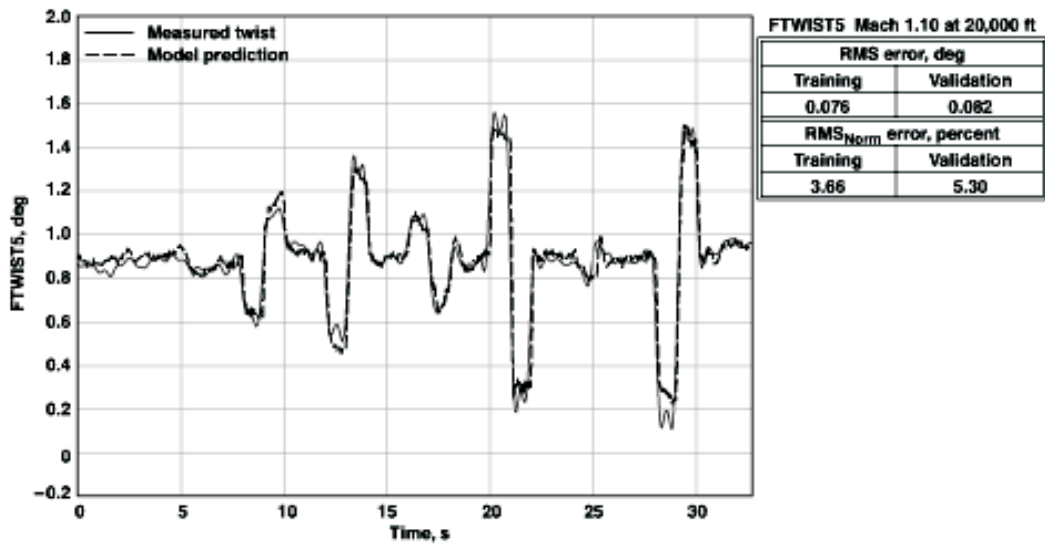| RMS_Norm error, percent	
Training	Validation
4.14	6.43

(a) FTWIST3 time history.

Figure 12: Mach 1.10 at an altitude of 20,000 ft total error and medium differential doublets plot.

FTWIST4 Mach 1.10 at 20,000 ft

RMS error, deg	
Training	Validation
0.088	0.085
RMS$_{Norm}$ error, percent	
Training	Validation
2.78	7.15

(b) FTWIST4 time history.

FTWIST5 Mach 1.10 at 20,000 ft

RMS error, deg	
Training	Validation
0.076	0.082
RMS$_{Norm}$ error, percent	
Training	Validation
3.66	5.30

(c) FTWIST5 time history.

FTWIST6 Mach 1.10 at 20,000 ft

RMS error, deg	
Training	Validation
0.096	0.106
RMS$_{Norm}$ error, percent	
Training	Validation
4.00	6.15
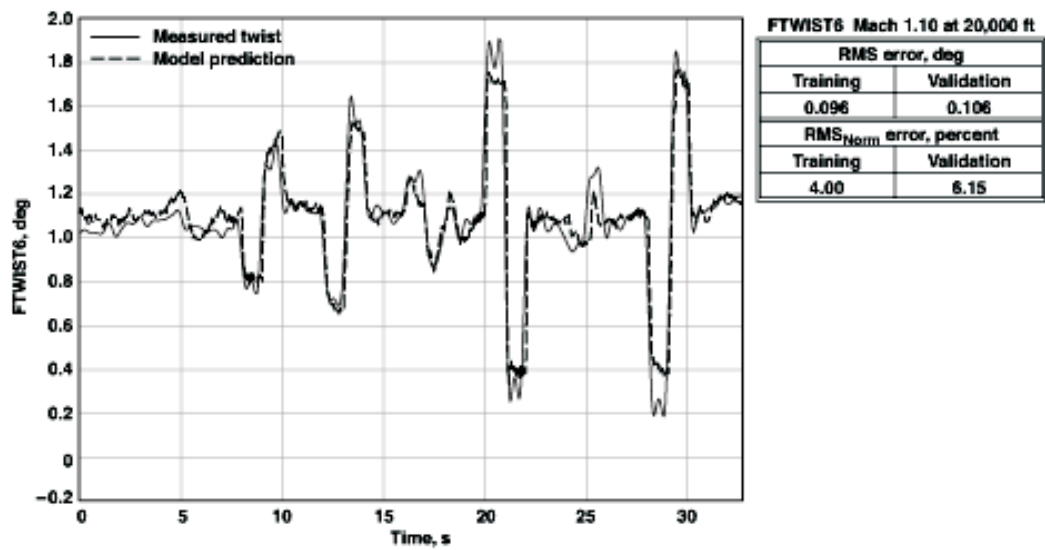
(d) FTWIST6 time history.
Figure 12: Concluded.

13

Considerably more maneuvers comprised subsonic flight conditions. This ultimately led to higher quality models than those at supersonic conditions. The optimal subsonic and supersonic results occurred at Mach 0.85 at an altitude of 5,000 ft and Mach 1.10 at an altitude of 20,000 ft, respectively, based on the average errors from all four twist stations. Higher dynamic pressure conditions produced higher errors as shown at Mach 0.95 at an altitude of 5,000 ft and Mach 1.20 at an altitude of 15,000 ft. The most consistent station to model was FTWIST5, whereas FTWIST4 proved to have significant nonlinearities. These inaccuracies may be the result of aerodynamically induced control-surface deformation or poor twist resolution discussed previously. Control-surface aeroelasticity most likely contributes a large roll in twist model error and is a topic for another study.

As mentioned previously, maneuvers other than OBES doublets were used to develop each model. Figure 13 illustrates a typical 45-deg bank-to-bank maneuver using 23-percent lateral stick deflection. The graph shows the wingtip-measured twist original model prediction and DPA prediction. In nearly all of the six flight conditions used to create DPA, original model results compared more closely with actual twist measurements. Table 6 shows similar RMS and RMS_{Norm} error analysis for the DPA results. Also added to the table are an interpolated (Mach 1.25 at an altitude of 20,000 ft) and an extrapolated (Mach 1.20 at an altitude of 15,000 ft) flight condition. Neither condition was used in formation of the DPA; however, the dynamic pressure of Mach 1.25 at an altitude of 20,000 ft is valid for the assumption. Figure 14 shows measured and predicted twist results of a half stick 360-deg roll from the interpolated condition. Dynamic pressure from Mach 1.20 at an altitude of 15,000 ft fell outside the valid range and proved difficult to improve with the DPA. These results suggest the original model will produce superior results at specified flight conditions and the DPA provides reasonably accurate twist predictions to be monitored between specific flight conditions.

	RMS error, deg			RMS_{Norm} error, percent	
	Training	Validation		Training	Validation
130m25k	0.130	0.167		6.46	9.83
130m20k	0.101	0.082		6.10	6.19
125m20k*	0.106	0.068		5.77	4.83
120m25k	0.169	0.084		7.23	4.77
120m20k	0.095	0.080		4.71	4.30
120m15k**	0.261	0.092		14.27	6.26
110m25k	0.148	0.080		5.74	4.89
110m20k	0.110	0.106		4.56	6.56

  * Interpolated flight condition.   ** Extrapolated flight condition.
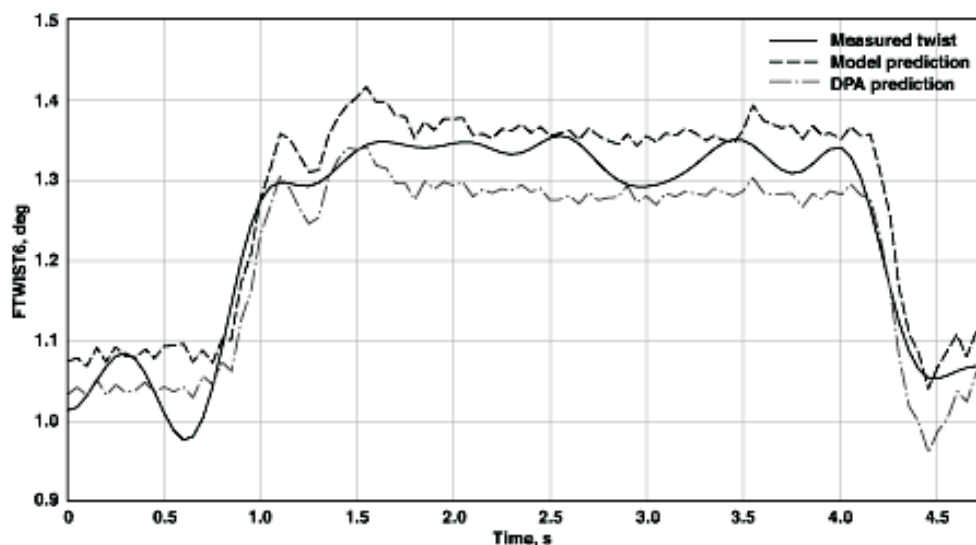
Table 6: DPA results.

Figure 13: Mach 1.10 at an altitude of 25,000 ft, 4-deg bank-to-bank (23-percent lateral stick).
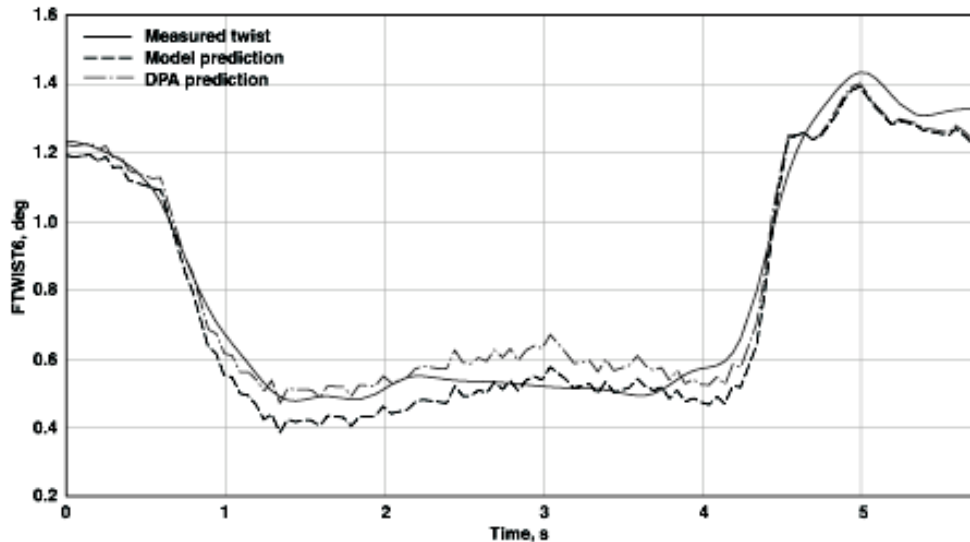
14

Figure 14: Mach 1.25 at an altitude of 20,000 ft, 360-deg roll (50-percent lateral stick) interpolation.

6   CONCLUDING REMARKS

In summary, a model to predict the elastic streamwise wing twist on the active aeroelastic wing aircraft was developed to examine wing twist in the simulator, understand aircraft performance uncertainties, and assist with computational fluid dynamic and aeroelastic model development. Documentation included the instrumentation and flight data background, data acquisition, signal conditioning process, and linear regression method used to create the original model. Further model development incorporated the use of a dynamic pressure-based assumption. Illustrative results were presented at various flight conditions and twist stations.

Original model results showed an explicit linear relationship between control-surface positions and aircraft state variables with wing twist. Typically, the most challenging flight conditions to predict were high in dynamic pressure or closer to the transonic region. Twist station 4 gave the highest overall original model prediction error, most likely a result of high deflection and twist resolution output of the two targets. Twist station 5 returned the lowest error overall, probably a result of the low deflection and twist resolution. Results from the dynamic pressure assumption suggest that the original model will produce superior results at specified flight conditions, and dynamic pressure assumption provides reasonably accurate twist predictions to be monitored between specific flight conditions. Further study into usefulness of a similar subsonic equation may prove useful. Indications of nonlinearity were present in some of the data.

7   REFERENCES

[1]   DeAngelis, V. Michael and Robert Fodale, *"Electro-Optical Flight Deflection Measurement System,"* 18th Annual Symposium Society of Flight Test Engineers Proceedings, Paper 22, September 28–October 2, 1987.

[2]   Pendleton, Edmund W., Denis Bessette, Peter B. Field, Gerald D. Miller, and Kenneth E. Griffin, "Active Aeroelastic Wing Flight Research Program: Technical Program and Model Analytical Development," *Journal of Aircraft*, Vol. 37, No. 4, July–August 2000.

[3]   Lokos, William A., *"Predicted and Measured In-Flight Wing Deformations of a Forward-Swept-Wing Aircraft,"* 21st Annual Symposium Society of Flight Test Engineers Proceedings, Paper A92-35926 14-01, August 6–10, 1990.

[4] DeAngelis, V. M., "*In-Flight Deflection Measurement of the HiMAT Aeroelastically Tailored Wing*," AIAA/SETP/SFTE/SAE/ITEA/IEEE 1st Flight Testing Conference, Las Vegas, Nevada, AIAA-81-2450, November 11–13, 1981.

[5] Powers, Sheryll Goecke, Lannie D. Webb, Edward L. Friend, and William A. Lokos, *Flight Test Results From a Supercritical Mission Adaptive Wing With Smooth Variable Camber*, NASA TM-4415, 1992.

[6] Bonnema, Kenneth L. and William A. Lokos, "*AFTI/F-111 Mission Adaptive Wing Flight Test Instrumentation Overview*," 35th International Instrumentation Symposium, Orlando, Florida, Paper No. 89-0084, May 1–4, 1989.

[7] Lokos, William A., Catherine M. Bahm, and Robert A. Heinle, *Determination of Stores Pointing Error Due to Wing Flexibility Under Flight Load*, NASA TM-4646, 1995.

[8] Iliff, Kenneth W. and Kon-Sheng Charles Wang, *Flight-Determined Subsonic Lateral-Directional Stability and Control Derivatives of the Thrust-Vectoring F-18 High Angle of Attack Research Vehicle (HARV), and Comparisons to the Basic F-18 and Predicted Derivatives*, NASA/TP-1999-206573, 1999.

[9] Iliff, Kenneth W. and Kon-Sheng Charles Wang, *Flight-Determined Subsonic Longitudinal Stability and Control Derivatives of the F-18 High Angle of Attack Research Vehicle (HARV) With Thrust Vectoring*, NASA/TP-97-206539, 1997.

[10] Lokos, William A. and Rick Stauf, *Strain-Gage Loads Calibration Parametric Study*, NASA/TM-2004-212853, 2004.